DOI:
10.1016/j.jocs.2017.07.013

Document Version
Peer reviewed version

Title: Estimating cardiac contraction through high resolution data assimilation of a personalized mechanical model

Author: Henrik Finsberg Gabriel Balaban Stian Ross Trine F. Håland Hans Henrik Odland Joakim Sundnes Samuel Wall

PII: S1877-7503(17)30819-0
DOI: http://dx.doi.org/doi:10.1016/j.jocs.2017.07.013
Reference: JOCS 728

To appear in:

Received date: 22-12-2016
Revised date: 2-6-2017
Accepted date: 16-7-2017

Please cite this article as: Henrik Finsberg, Gabriel Balaban, Stian Ross, Trine F. Håland, Hans Henrik Odland, Joakim Sundnes, Samuel Wall, Estimating cardiac contraction through high resolution data assimilation of a personalized mechanical model, <*![CDATA[Journal of Computational Science]]*> (2017), http://dx.doi.org/10.1016/j.jocs.2017.07.013

Estimating cardiac contraction through high resolution data assimilation of a personalized mechanical model

Henrik Finsberg[a,b,d,1,*], Gabriel Balaban[f], Stian Ross[c,d], Trine F. Håland[c,d], Hans Henrik Odland[c,d], Joakim Sundnes[a,b,d], Samuel Wall[a,e,d]

[a] *Simula Research Laboratory, P.O. Box 134 1325 Lysaker, Norway*
[b] *Department of Informatics, University of Oslo, P.O. Box 1080, Blindern 0316 Oslo, Norway*
[c] *Faculty of Medicine, University of Oslo, P.O. Box 1078 Blindern, 0316 Oslo, Norway*
[d] *Center for Cardiological Innovation, Songsvannsveien 9, 0372 Oslo, Norway*
[e] *Department of Mathematical Science and Technology, Norwegian University of Life Sciences, Universitetstunet 3 1430 s, Norway*
[f] *Department of Imaging Sciences and Bioengineering, King's College London, St. Thomas Hospital, Westminster Bridge Rd, Lambeth, London SE1 7EH, UK*

Abstract

Cardiac computational models, individually personalized, can provide clinicians with useful diagnostic information and aid in treatment planning. A major bottleneck in this process can be determining model parameters to fit created models to individual patient data. However, adjoint-based data assimilation techniques can now rapidly estimate high dimensional parameter sets. This method is used on a cohort of heart failure patients, capturing cardiac mechanical information and comparing it with a healthy control group. Excellent fit ($R^2 \geq 0.95$) to systolic strains is obtained, and analysis shows a significant difference in estimated contractility between the two groups.

Keywords:

Cardiac Mechanics, Adjoint Method, Data assimilation, PDE-constrained optimization, Contractility

1. Introduction

Patient-specific cardiac modeling has emerged as a potential tool for clinical diagnosis as well as treatment optimization[1]. By linking patient measurements to physical processes through a mathematical framework, models can provide us with additional insight into cardiac function or dysfunction at the level of the individual. However, the complexity of the heart makes this difficult, and this is recognized as a key challenge in modern bioengineering [2].

*Corresponding author
Email address: henriknf@simula.no (Henrik Finsberg)

One difficulty is the effort to personalize models and simulations to individual patients. While a wealth of clinical data exists to parameterize such 'patient-specific' models, methods to assimilate this data into simulations can involve extensive computation time, often putting them outside the scope of clinical utility. However, new methods are emerging to improve the flow of clinical measurements into powerful data driven simulations. Automated geometry segmentation [3] and improved optimization techniques [4], can improve the speed at which patient-specific models can be built and parameterized. In particular, recent advancements in adjoint-based data assimilation techniques [5] offer an efficient way to assimilate ventricular mechanical information using highly spatially resolved parameters.

Here we use an adjoint based assimilation method with a mechanical model in order to construct simulations that accurately reflect clinical motion data, both for healthy controls and patients suffering from left bundle branch block (LBBB). The use of a highly spatially resolved contraction parameter, enabled through adjoint-methods, provides excellent data fit to measured strains and volumes, and fit models provide estimates of cardiac contraction. Such biomarkers may prove useful to clinicians for diagnoses of problems with cardiac function, and to better plan therapies.

2. Materials and methods

2.1. Data acquisition

Clinical measurements of cardiac function for seven LBBB patients were obtained from the Impact study [6]. Data was also acquired for seven healthy volunteers. 4D echocardiographic images of the left ventricle (LV), for both the LBBB patients and healthy subjects, were captured using a GE Vingmed E9 device, and analysis carried out with the software package EchoPac. For each subject, depending on frame rate and cardiac cycle time, the analysis provided between 15 and 50 LV volumes, geometric segmentations of the LV endocardium and epicardium, and cardiac strain calculated via speckle tracking. The strain were defined according to the 17 segment AHA-zone representation [7], in the longitudinal, radial and circumferential direction, giving a total of 51 strain measurements per time point, with the reference time point for strain analysis being the first frame after onset of QRS.

The LBBB patients had LV pressure measurements taken during implantation of a cardiac resynchronization therapy (CRT) device, and valvular events were used to synchronize the pressure to the echo data. In the healthy control group, where invasive pressure measurements were absent, the pressure waveform from one of the LBBB

patients was used and scaled to reported values of the end-diastolic and end-systolic left ventricular pressure [Table 30-1 in [8]].

2.2. Automated geometry and microstructure creation

For each patient, a 3D tetrahedral mesh of the LV was constructed from triangulated segmented surfaces of the endo- and epicardium corresponding to the frame at the beginning of atrial systole, Figure 1. A cut was made at the ventricular base of the segmentation, so that the mesh cavity volume and the ultrasound measured volume differed by less than 1 ml. Mesh cells were marked into the 17 AHA regions through the regionally delineated strain data, and the myocardial fiber orientation, denoted by $\mathbf{f}_0$, were assigned using the algorithm from Bayer et al [9], with the endo- and epicardial helix fiber angles set to $\alpha_{\text{endo}} = 60$ and $\alpha_{\text{epi}} = -60$, respectively.

2.3. Mechanical Model

We represent the heart as a hyperelastic continuum body, where the coordinates in the reference ($\mathbf{X}$) and the current ($\mathbf{x}$) configuration are related via the displacement field $\mathbf{u} = \mathbf{x} - \mathbf{X}$. Furthermore, we utilize the deformation gradient, the determinant of the deformation gradient and, the right Cauchy-Green deformation tensor given by $\mathbf{F} = \mathbf{I} + \nabla\mathbf{u}$, $J = \det \mathbf{F}$ and $\mathbf{C} = \mathbf{F}^T\mathbf{F}$, respectively. To model the passive behavior of the myocardium, the transversely isotropic strain energy function proposed in [10] is adopted:

$$\mathcal{W}(I_1, I_{4\mathbf{f}_0}) = \frac{a}{2b}\left(\exp\left\{b(I_1 - 3)\right\} - 1\right) + \frac{a_f}{2b_f}\left(\exp\left\{b_f(I_{4\mathbf{f}_0} - 1)_+^2\right\} - 1\right). \tag{1}$$

Here $I_1 = \operatorname{tr}\mathbf{C}$ and $I_{4\mathbf{f}_0} = \mathbf{f}_0 \cdot (\mathbf{C}\mathbf{f}_0)$ are invariants of $\mathbf{C}$, $(\cdot)_+ = \max\{\cdot, 0\}$, and a, a_f, b, b_f are material stiffness parameters defining the elastic properties of the myocardium. We follow a common approach and assume that the myocardium is incompressible. Incompressibility is incorporated in the model by using a two-field variational approach, where we introduce a Lagrange multiplier p which represents the hydrostatic pressure, and the term $p(J - 1)$ is added to the strain-energy.

To model the active response we apply the approach of active strain [11], which is based on decomposing the deformation gradient into active and passive contributions, $\mathbf{F} = \mathbf{F}_e\mathbf{F}_a$. We choose $\mathbf{F}_a = (1-\gamma)\mathbf{f}_0 \otimes \mathbf{f}_0 + \frac{1}{\sqrt{1-\gamma}}(\mathbf{I} - \mathbf{f}_0 \otimes \mathbf{f}_0)$, where γ is a parameter that represents the relative active shortening along the fibers. For reference, we have also

performed tests with the commonly used active stress formulation, where the stress tensor is additively decomposed into active and passive stress $\sigma = \sigma_p + \sigma_a$. Here σ_p is the elastic material response, and $\sigma_a = T_a \mathbf{f} \otimes \mathbf{f}$ with $\mathbf{f} = \mathbf{F}\mathbf{f}_0$ and T_a a scalar variable representing active fiber tension.

For both approaches, the resulting displacement field $\mathbf{u}$ and hydrostatic pressure p are determined by using the principle of stationary potential energy [12], which is based on minimizing the total energy $\Pi(\mathbf{u}, p)$, which includes internal energy derived from (1) and external energy. The external energy includes contributions from the measured cavity pressure p_{LV}, and a linear spring term at the basal boundary, with spring constant $k = 10.0$ kPa. The equilibrium solution is found by solving for the minimum potential energy, $\delta\Pi(\mathbf{u}, p) = 0$.

2.4. Data Assimilation

In order to constrain the model to each patient's clinical measurements, we consider a PDE-constrained optimization problem where the objective functional is given by the misfit between simulated and measured strain and volume along with a first order Tikhonov regularization of the model parameters.

$$\begin{aligned} \underset{m}{\text{minimize}} \quad & \alpha\left(\frac{V^i - \tilde{V}^i}{V^i}\right)^2 + (1-\alpha)\sum_{j=1}^{17}\sum_{k\in\{c,r,l\}}\left(\varepsilon_{kj}^i - \tilde{\varepsilon}_{kj}^i\right)^2 + \lambda\|\nabla m^i\|^2 \\ \text{subject to} \quad & \delta\Pi(\mathbf{u}, p) = 0. \end{aligned} \tag{2}$$

Here V and ε_{kj} are the measured volume and regional Lagrangian strain in segment j in direction k respectively, and $\tilde{V}^i = -\frac{1}{3}\int_{\partial\Omega_{\text{endo}}}(\mathbf{X}+\mathbf{u})\cdot J\mathbf{F}^{-T}\mathbf{N}\mathrm{d}S$, and $\varepsilon_{kj} = \frac{1}{|\Omega_j|}\int_{\Omega_j}\mathbf{e}_k^T\nabla\mathbf{u}\,\mathbf{e}_k\mathrm{d}x$. The parameters α and λ control the weights on the different terms, and the sum in the second term is taken over the seventeen AHA segments, and the three different strain components (Section 2.1).

The data assimilation procedure is divided into two phases; a passive and an active phase. For the passive phase we iteratively estimate the unloaded configuration and the linear isotropic parameter, a in (1), using an algorithm similar to the one described in [13], and we set $\alpha = 1.0$, with $\lambda = 0$ and $\gamma = 0$, minimizing only the misfit with the measured volumes. The remaining material parameters are fixed according to [Table 1 row 3 of [10]]. For the active phase we fix the material parameter optimized in the passive phase, choose the control variable m to be γ or T_a for the active strain and active stress model respectively, and set $\alpha = 0.95$ and $\lambda = 0.01$. This choice of α and λ was based on the analysis done in [5]. A summary of our optimization pipeline is provided to the right in Figure 1.

2.5. Implementation details

We employ a Galerkin finite element method with Taylor-Hood tetrahedral elements, that is $(\mathbf{u}, p) \in \mathbb{P}_2 \times \mathbb{P}_1$, with $\mathbb{P}_n$ being the space of piecewise polynomials of degree n. The solver is implemented in the finite element framework FEniCS [14], and uses a Newton trust region algorithm [15] to solve nonlinear systems. The minimization of the model-data misfit functional (2) is accomplished by a sequential quadratic programming algorithm (SQP) [16], where the functional gradient is computed by solving an automatically derived adjoint equation [17]. In these minimizations an upper bound of 0.5 and 500 kPa is set for the active strain (γ) and active stress (T_a) control variable respectively, which both are modeled as functions in $\mathbb{P}_1$, yielding one parameter per nodal point in the mesh.

2.6. Contraction analysis

Although direct physical interpretation of the active strain parameter γ is difficult, it may be seen as the relative shortening of an isolated and unloaded muscle cell. A high value of γ is therefore an indication of higher contractile force in the myocardium, independent of load. We propose that the spatially averaged γ over the entire LV, denoted by $\overline{\gamma}$, can be used as an index of global contractility. Similarly, the active stress parameter T_a is related to force development at level of the sarcomeres[18], and the spatially averaged T_a, denoted $\overline{T_a}$ can be used as an index of contractility. In addition to the contractility information contained in $\overline{\gamma}$ and $\overline{T_a}$, the overall elastic state of the optimized patient models can be used to give estimates of LV elastance. The left ventricular end-systolic elastance E_{ES}, the response of end systolic volume to increased load, is considered to be one of the major determinants for cardiac systolic function, and was in [19] proposed as a global index of ventricular contractility. It is possible to estimate the end systolic elastance directly if the end systolic pressure is known or estimated, by perturbing the loading conditions on the optimized model at end systole while fixing the remaining quatities, and calculating the slope in the resulting ES pressure-volume curve. More precisely, if $p_{\mathrm{lv}}^{\mathrm{ES}}$ is the end-systolic ventricular pressure, with cavity volume V^{ES}, we change the pressure to $p_{\mathrm{lv}}^{\mathrm{ES}+\Delta} = p_{\mathrm{lv}}^{\mathrm{ES}} + \Delta p_{\mathrm{lv}}$, resulting in a change in volume, $V^{\mathrm{ES}+\Delta} = V^{\mathrm{ES}} + \Delta V$. The estimate of end-systolic elastance can then be calculated by

$$\tilde{E}_{\mathrm{ES}} = \frac{\Delta p_{\mathrm{lv}}}{\Delta V}. \tag{3}$$

3. Results and discussion

3.1. Matching of strain and volume

We show the results from two representative simulations in Figure 2, one from the LBBB group and one from the healthy control group. Snapshots from the calculated unloaded and end-systolic configurations are depicted. For the unloaded geometry, we also show the image-based geometry at beginning of atrial systole, and for the end-systolic configuration we show the longitudinal strain using both the active stress and active strain approach. We also show the agreement with the corresponding PV-loops.

The total analysis of the 14 patients involved optimizing 432 volume measurements and 20 853 strain measurements. The average time for one forward and gradient evaluation was 8.3 and 8.9 seconds respectively when running on a cluster using four cores, with an average number of control parameters being 985.

In order to visualize the overall match of simulated to measured data, we show linear regression plots in Figure 3. These results are all based on the active strain formulation. For the strain, we separately consider the diastolic and systolic points, as different types of data were used to constrain the model in these two phases, namely volume in the diastolic phase and strain in the systolic phase. An excellent overall fit was obtained for the optimized volume ($R^2 = 1.00$) and systolic strains ($R^2 = 0.95$). Diastolic strains, not used in the optimization, were less well matched ($R^2 = 0.31$).

3.2. Estimation of global contractility and elastance

Global contraction time courses, $\overline{\gamma}$ and $\overline{T}_a$, for each patient were synchronized to the valvular events to normalize for differing cycle lengths. The average and standard deviation of these normalized traces for the LBBB vs the healthy controls are shown in left of Figure 4. The healthy patients had a much higher level of contraction through the cardiac cycle, and the peak values were compared using one-way ANOVA, yielding a $P-$value less than 0.001 for both the active strain and the active stress approach.

The values of calculated $\tilde{E}_{\text{ES}}$ for the healthy and LBBB patients are shown to the right in Figure 4. The calculated elastances of the LBBB group were significantly lower than for the healthy group, with the comparison between the groups using one-way ANOVA giving a $P-$value of 0.009 and 0.003 for the active strain and active stress respectively.

4. Discussion

In this study we applied an adjoint-based data assimilation technique to constrain patient data to a cardiac mechanics model. LV pressure was used as a boundary condition, and an unloading algorithm was used to find a reference geometry and a material parameter based on diastolic P-V measurements. Active contraction was then captured by assimilation of measured systolic LV regional strains by the means of a spatially varying contraction parameter. We tested this methodology on a group of seven healthy control patients and seven patients diagnosed with LBBB. The results gave an excellent fit between the measured and simulated volume and systolic strain ($R^2 \geq 1.00$ and $R^2 \geq 0.95$, respectively) for more than 21,000 observation points. Meanwhile diastolic strains, due to the quality of the strain measurements during late diastole, were not included in the optimization and had a resulting poor fit. However, allowing for spatial heterogeneity in the material parameters and/or optimizing more parameters from the material model, could allow for better fit values also in this part of the cycle and will be further investigated. Of course, questions regarding uniqueness of such solutions in general will need to be carefully addressed in future studies.

Our simulations show that estimating the unloaded configuration may be important to capture the correct material parameters, as we optimized to a consistently softer material when the unloading algorithm was used. Meanwhile, this seemed to have less of an impact in systole, as the the overall estimated ventricular elastance was unchanged.

These calibrated models allow for estimating aspects of cardiac contractility, such as the traditional measure of end-systolic elastance, by perturbations of the model at the end systolic configuration. The healthy control group had significantly higher estimated end-systolic elastance than the LBBB group, although limitations exist with these calculations due to using a synthetic pressure curve with the healthy group. However, the values calculated by using direct pressure readings for the LBBB group (3 - 10 mmHg) are slightly higher but correspond very well with the range provided for a heart failure cohort of (0.5 - 4.9 mm Hg) [20]. Clinically, end systolic elastance is measured based on data obtained using multiple beats subjected to different loading conditions. This change in loading conditions also gives rise to changes in the active tension as a function of myocardial strain, an effect that is not modelled directly here. Therefore, although we can calculate a discriminating marker of stiffness between the two cohorts, future work evaluating this method over a number of beats with different loading conditions is needed to assess its relation to clinical end-systolic elastance.

In addition to the end-systolic elastance estimates, our simulations also were used to compare the average value of γ and T_a, which may also be interpreted as indices of contractility, between the two groups through the cardiac cycle. Again, the healthy controls showed a significantly higher peak values of active strain and stress, compared to the LBBB group and both analysis methods showed comparable trends.

5. Conclusions

Adjoint-based data assimilation is a powerful technique for estimating high dimensional parameters in order to incorporate large amounts of information into a model. Although limitations in our patient data and assumptions remain, we have demonstrated how such techniques can be applied to problems in mechanics for use in extracting potential biomarkers related to cardiac contractility. Future work will be used to adjust and improve such models and work towards their validation and clinical utility.

Acknowledgments

This study was funded by Research Council of Norway: Center for Biomedical Computing at Simula Research Laboratory and Center for Cardiological Innovation at Oslo University Hospital. Computations were performed on the Abel supercomputing cluster at the University of Oslo via a Notur project.

References

[1] M. Viceconti, P. Hunter, The virtual physiological human: Ten years after, Annual Review of Biomedical Engineering 18 (1).

[2] P. Hunter, P. V. Coveney, B. de Bono, V. Diaz, J. Fenner, A. F. Frangi, P. Harris, R. Hose, P. Kohl, P. Lawford, et al., A vision and strategy for the virtual physiological human in 2010 and beyond, Philosophical Transactions of the Royal Society of London A: Mathematical, Physical and Engineering Sciences 368 (1920) (2010) 2595–2614.

[3] S. I. Rabben, Technical principles of transthoracic three-dimensional echocardiography, in: Textbook of Real-Time Three Dimensional Echocardiography, Springer, 2010, pp. 9–24.

[4] R. Chabiniok, P. Moireau, P.-F. Lesault, A. Rahmouni, J.-F. Deux, D. Chapelle, Estimation of tissue contractility from cardiac cine-MRI using a biomechanical heart model, Biomechanics and modeling in mechanobiology 11 (5) (2012) 609–630.

[5] G. Balaban, H. Finsberg, H. H. Odland, M. Rognes, S. Ross, J. Sundnes, S. Wall, High resolution data assimilation of cardiac mechanics applied to a dyssynchronous ventricle, International Journal for Numerical Methods in Biomedical Engineering.

[6] O. U. Hospital, Acute feedback on left ventricular lead implantation location for cardiac resynchronization therapy (CCI impact), https://clinicaltrials.gov (2016).

[7] M. D. Cerqueira, N. J. Weissman, V. Dilsizian, A. K. Jacobs, S. Kaul, W. K. Laskey, D. J. Pennell, J. A. Rumberger, T. Ryan, M. S. Verani, et al., Standardized myocardial segmentation and nomenclature for tomographic imaging of the heart a statement for healthcare professionals from the cardiac imaging committee of the council on clinical cardiology of the american heart association, Circulation 105 (4) (2002) 539–542.

[8] M. E. Klingensmith, et al., The Washington manual of surgery, Lippincott Williams & Wilkins, 2008.

[9] J. Bayer, R. Blake, G. Plank, N. Trayanova, A novel rule-based algorithm for assigning myocardial fiber orientation to computational heart models, Annals of biomedical engineering 40 (10) (2012) 2243–2254.

[10] G. A. Holzapfel, R. W. Ogden, Constitutive modelling of passive myocardium: a structurally based framework for material characterization, Philosophical Transactions of the Royal Society of London A: Mathematical, Physical and Engineering Sciences 367 (1902) (2009) 3445–3475.

[11] D. Ambrosi, S. Pezzuto, Active stress vs. active strain in mechanobiology: constitutive issues, Journal of Elasticity 107 (2) (2012) 199–212.

[12] G. A. Holzapfel, Nonlinear solid mechanics, Vol. 24, Wiley Chichester, 2000.

[13] A. Nikou, S. M. Dorsey, J. R. McGarvey, J. H. Gorman III, J. A. Burdick, J. J. Pilla, R. C. Gorman, J. F. Wenk, Effects of using the unloaded configuration in predicting the in vivo diastolic properties of the heart, Computer methods in biomechanics and biomedical engineering 19 (16) (2016) 1714–1720.

[14] A. Logg, K.-A. Mardal, G. Wells, Automated solution of differential equations by the finite element method: The FEniCS book, Vol. 84, Springer Science & Business Media, 2012.

[15] S. Balay, J. Brown, K. Buschelman, W. Gropp, D. Kaushik, M. Knepley, L. C. McInnes, B. Smith, H. Zhang, PETSc web page, http://www.mcs.anl.gov/petsc (2015).

[16] D. Kraft, et al., A software package for sequential quadratic programming, DFVLR Obersfaffeuhofen, Germany, 1988.

[17] P. E. Farrell, D. A. Ham, S. W. Funke, M. E. Rognes, Automated derivation of the adjoint of high-level transient finite element programs, SIAM Journal on Scientific Computing 35 (4) (2013) C369–C393.

[18] S. Göktepe, A. Menzel, E. Kuhl, The generalized hill model: A kinematic approach towards active muscle contraction, Journal of the Mechanics and Physics of Solids 72 (2014) 20–39.

[19] K. Sagawa, H. Suga, A. A. Shoukas, K. M. Bakalar, End-systolic pressure/volume ratio: a new index of ventricular contractility, The American journal of cardiology 40 (5) (1977) 748–753.

[20] H. Senzaki, C.-H. Chen, D. A. Kass, Single-beat estimation of end-systolic pressure-volume relation in humans a new method with the potential for noninvasive application, Circulation 94 (10) (1996) 2497–2506.

List of Figures

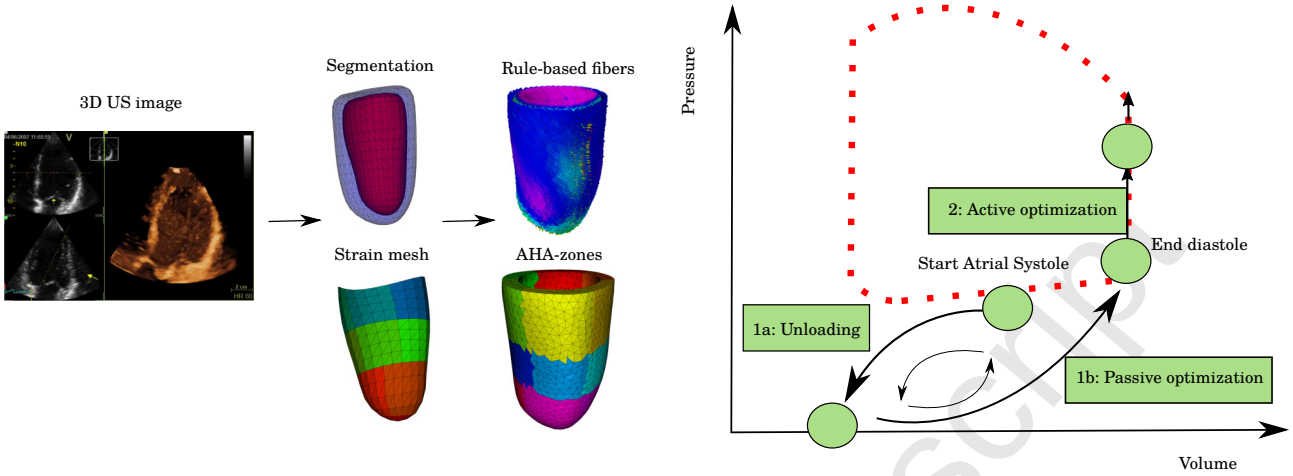

Figure 1: Left: Automated anatomical modeling pipeline to produce AHA marked simulation meshes with applied fiber orientations from 3D echocardiographic segmentations. Right: Optimization pipeline. 1. Unloaded geometry and the linear isotropic material parameter a in (1) are estimated iteratively. The unloaded geometry is estimated based on the backward displacement method (1a) [13] and a is estimated by minimizing the difference between simulated and measured volumes (1b). 2. The unloaded geometry and the material properties are fixed, and the amount of contraction (γ for active strain and T_a for active stress) is estimated by minimizing the mismatch between simulated and measured strain and volume. The active optimization continues to the next measurement point until all measurement points in the cycle are covered.

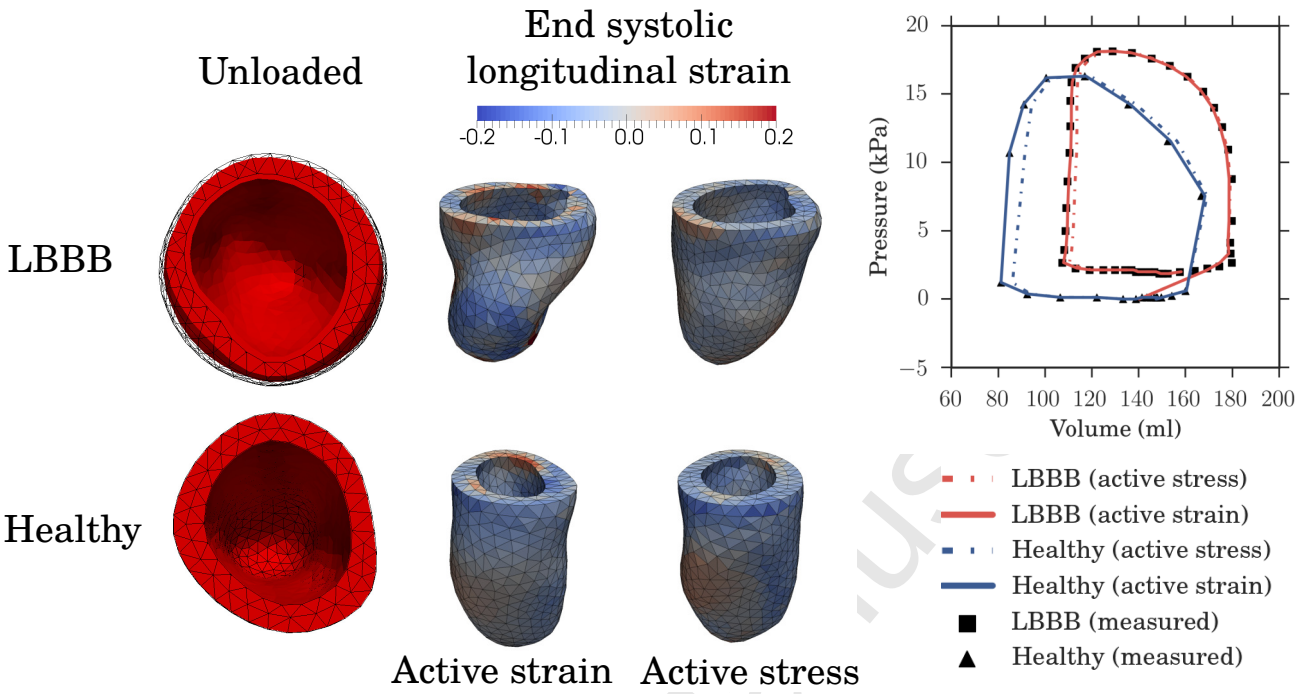

Figure 2: Left: Snap shots of the unloaded geometry in red, and the corresponding image based geometry taken at beginning of atrial systole in black wire-frame. Middle: Snap shot of end systolic configurations using the active strain and active stress approach. Color-map shows the end-systolic longitudinal strain. Right: Simulated and measured pressure-volume loops for these hearts using the active strain and active stress approach.

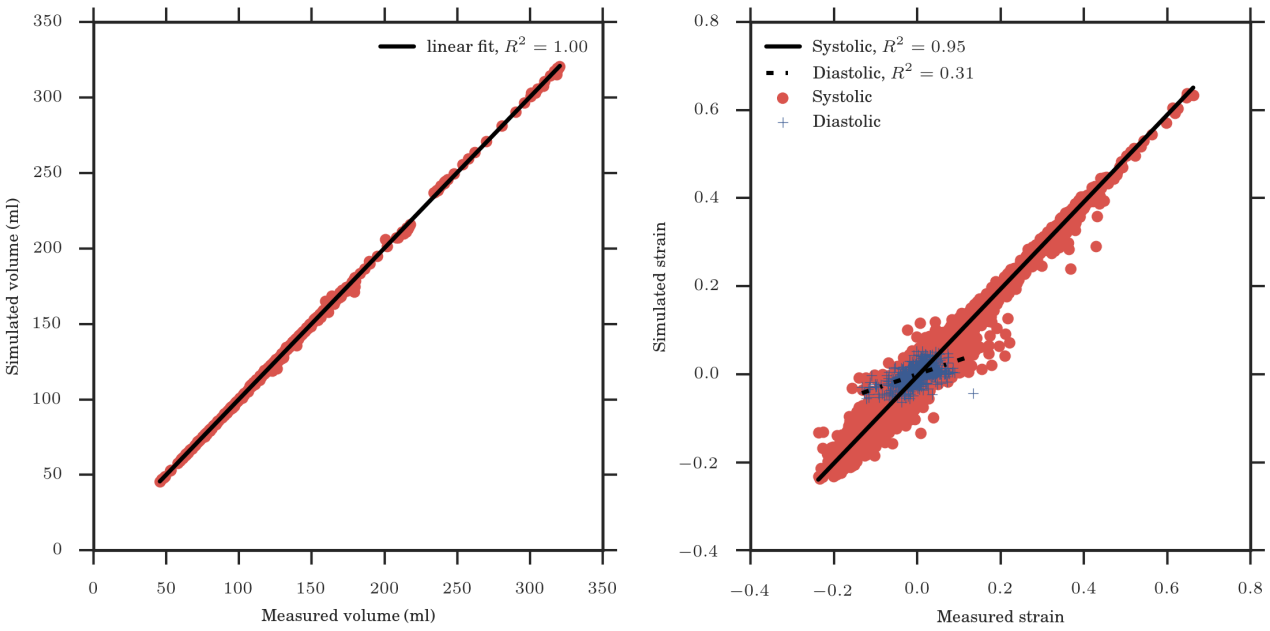

Figure 3: Scatter plot of simulated (y-axis) and measured (x-axis) strain and volume using the active strain approach. Left: Scatter plot of simulated versus measured volumes and the best linear least-squares fit of these points, (slope = 1.00). Right: Scatter plot of simulated versus measured strain for all segments and all directions, separated into the diastole, were only the volume was optimized and systole, where both the strain and volume were optimized. For diastole, the slope of the best linear fit was 0.31, while the best linear fit for the systolic points had a slope of 0.95.

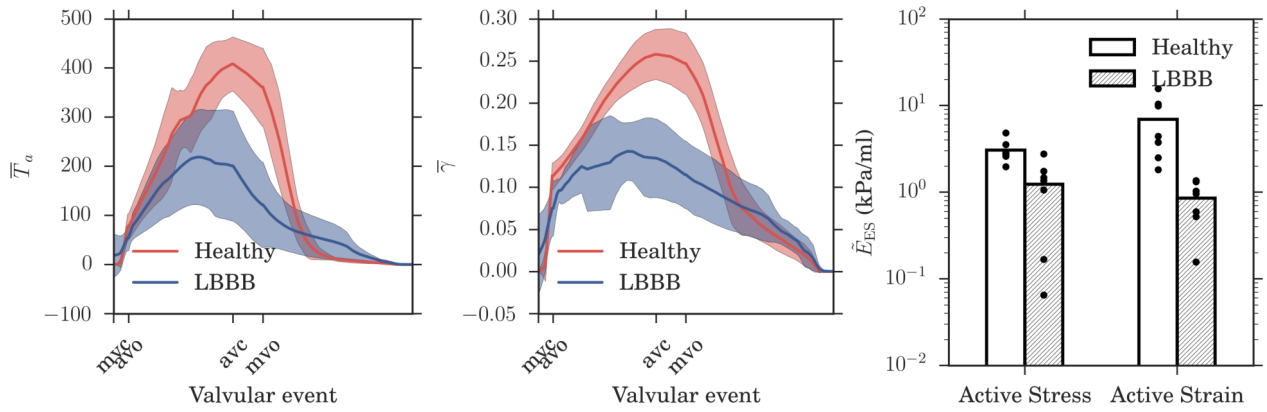

Figure 4: Extracted biomarkers related to cardiac contractility. Left: Mean value of T_a for the two groups synchronized with respect to valvular events (mvc: mitral valve closure, avo: aortic valve opening, avc: aortic valve closure, mvo: mitral valve opening). Shaded region shows ± one standard deviation. Middle: Mean value of γ for the two groups synchronized with respect to the same valvular events. Right: Estimated values of $\tilde{E}_{\mathrm{ES}}$, given by (3) using the active stress and the active strain approach. The mean value is depicted for each group as a bar, and individual points are also displayed.

- Adjoint based data assimilation of cardiac mechanics.
- Personalized simulations directly from cardiac ultrasound.
- Excellent fit with measured volumes and regional strains.
- Estimation of end systolic elastance and ventricular contraction.

Henrik Finsberg Henrik Finsberg graduated in 2014 after finishing a joint master degree in Applied and Engineering Mathematics at NTNU in Trondheim and DTU in Copenhagen. He is currently pursuing a Ph.D. at Simula Research Laboratory in the Center for Cardiological Innovation working with patient specific modeling of the heart. Areas of interests includes mathematical modeling, image analysis, visualization and geometric modeling.

Gabriel Balaban Gabriel Balaban is a post doctoral research fellow at King's College London currently working with modeling of cardiac electrophysiology. He did his doctoral studies at Simula Research Laboratory working with adjoint based data assimilation of cardiac mechanics.

Stian Ross Stian Ross, MD, is a board certified specialist in Internal Medicine and Cardiology. He started as a PhD student February 2014 in a clinical research program involving patients with chronic heart failure and dyssynchrony within the Center for Cardiological Innovation.

Trine F. Håland Trine Fink Håland, MD, is a board certified specialist in Internal Medicine and Cardiology. She started as a PhD fellow September 2013, working with patients with inherited cadiomyopathies/channelopathies. Her PhD research is focused on myocardial function and prediction of malignant arrhythmias in patients with hypertrophic cardiomyopathy by echocardiographic modalities.

Hans Henrik Odland Hans Henrik Odland, MD, did his doctoral studies at University of Oslo with Ph.D. thesis on non-invasive assessment of neonatal myocardial function. His research interests includes, non-invasive myocardial function assessment, bioimpedance and biofeedback, and force frequency relationships and assessment of contractility. He currently works at Oslo University Hospital as a consultant pediatric cardiologist and electrophysiologist.

Joakim Sundnes Joakim Sundnes is a Senior Research Scientist at Simula Research Laboratory and an Associate Professor at University of Oslo. He holds a Phd in Scientific Computing from the University of Oslo, and his main research interests are computational modeling of cardiac electrophysiology and mechanics.

Samuel Wall Samuel Wall is the head of the Cardiac Modeling (CaMo) group at Simula Research Laboratory and is an Associate Professor at the Norwegian University of Life Science. He received his Ph.D. in Bioengineering jointly from the University of California, Berkeley and the University of California, San Francisco and his work is focused on ventricular modeling of mechanical and electromechanical function of the heart.